Excitation-response relationships for linear structural systems with singular parameter matrices: A periodized harmonic wavelet perspective

G. D. Pasparakis[a], I. A. Kougioumtzoglou[b,*], V. C. Fragkoulis[a], F. Kong[c], M. Beer[a,d,e]

[a] *Institute for Risk and Reliability, Leibniz Universität Hannover, Callinstr. 34, 30167 Hannover, Germany*
[b] *Department of Civil Engineering and Engineering Mechanics, Columbia University, 500 W 120th Street, New York, NY 10027, USA*
[c] *School of Civil Engineering and Architecture, Wuhan University of Technology, China*
[d] *Institute for Risk and Uncertainty and School of Engineering, University of Liverpool, Liverpool L69 7ZF, UK*
[e] *International Joint Research Center for Engineering Reliability and Stochastic Mechanics, Tongji University, Shanghai, China*

Abstract

Novel wavelet-based input-output (excitation-response) relationships are developed referring to stochastically excited linear structural systems with singular parameter matrices. This is done by relying on the family of periodized generalized harmonic wavelets for expanding the excitation and response processes, and by resorting to the concept of Moore-Penrose matrix inverse for solving the resulting overdetermined linear system of algebraic equations to calculate the response wavelet coefficients. In this regard, system response statistics in the joint time-

*Corresponding author

Email addresses: george.pasparakis@irz.uni-hannover.de (G. D. Pasparakis), ikougioum@columbia.edu (I. A. Kougioumtzoglou), fragkoulis@irz.uni-hannover.de (V. C. Fragkoulis), kongfan@whut.edu.cn (F. Kong), beer@irz.uni-hannover.de (M. Beer)

November 27, 2021

frequency domain, such as the response evolutionary power spectrum matrix, can be determined in a straightforward manner based on the herein derived input-output relationships. The developed technique can be construed as a generalization of earlier efforts in the literature to account for singular parameter matrices in the governing equations of motion. The reliability of the technique is demonstrated by comparing the analytical results with pertinent Monte Carlo simulation data. This is done in conjunction with various diverse numerical examples pertaining to energy harvesters with coupled electromechanical equations, oscillators subject to non-white excitations modeled via auxiliary filter equations and structural systems modeled by a set of dependent coordinates.

Keywords: Evolutionary Power Spectrum, Moore-Penrose Matrix Inverse, Joint Time-Frequency Analysis, Random Vibration, Energy Harvesting

---

1. INTRODUCTION

Structural systems are often subjected to stochastic excitations exhibiting strong variations both in the time and the frequency domains [1]; thus, there is a need for developing efficient joint time-frequency analysis techniques for determining the time-varying frequency content of the system response. In this regard, various standard concepts and tools from random vibration theory have been generalized and extended over the past two decades based on wavelets; see [2, 3] for a broad perspective. These wavelet-based techniques have been widely employed for addressing diverse problems including, indicatively, system response analysis and statistics determination [4–6], system identification and damage detection [7–11], as well as evolutionary power spectrum (EPS) estimation [12–15].

Further, Spanos and co-workers employed the family of generalized harmonic wavelets (GHWs) for expanding the system excitation and response processes and for deriving an algebraic system of equations to be solved for the response process wavelet coefficients; and thus, for the response process EPS [16, 17]. Note that, compared to alternative wavelet families, a significant advantage of GHWs relates to the fact that they possess an additional coefficient that decouples the wavelet resolution in the frequency domain from the central frequency of the wavelet [18]. This means that the resolution of the wavelet analysis can be enhanced in frequency regions of interest. Clearly, this attribute renders GHWs an indispensable tool particularly for structural dynamics applications, where the interest lies typically in resonance phenomena manifesting themselves over relatively small regions in the frequency domain. Further, the technique has been extended to address multi-degree-of-freedom (MDOF) nonlinear systems [19], as well as systems endowed with fractional derivative terms [20].

More recently, Spanos and co-workers developed a novel GHW-based input-output relationship for determining the response EPS of linear systems [21], which circumvented the assumption of "local stationarity" inherent in the early developments in [16, 17, 19, 20] and yielded a higher degree of accuracy in predicting the system response. This was done by relying on a periodized version of GHWs for addressing the non-orthogonality of the GHW basis on a finite time interval, and by deriving interaction coefficients in closed form referring to wavelets at different scales and translation levels. Further, the technique was extended in [22] to account for nonlinear systems and in [23] to address systems with fractional derivative terms.

In this paper, the technique developed in [21] is further extended to account for MDOF systems exhibiting singular parameter matrices. This is done in conjunction with the concept of Moore-Penrose (MP) generalized matrix inverse for solving the resulting overdetermined linear system of algebraic equations and for computing the response wavelet coefficients and response EPS matrix. In passing, note that the herein derived input-output relationships can be construed as an enhancement of the respective ones in [24]. In fact, the range of applicability and the accuracy degree of the results in [24] are limited by the relatively strong assumption of local stationarity, which is removed in this paper. The reliability of the herein developed technique is demonstrated by comparing the analytical results with pertinent Monte Carlo simulation (MCS) data. This is done in conjunction with various diverse numerical examples exhibiting singular parameter matrices in the governing equations of motion. These include energy harvesters with coupled electromechanical equations, oscillators subject to non-white excitations modeled via auxiliary filter equations, and structural systems modeled by a set of dependent coordinates.

2. Mathematical formulation

2.1. Preliminaries: Periodized generalized harmonic wavelets

In general, wavelet-based solutions of differential equations governing the response of diverse systems necessitate the determination of coefficients representing the interactions between wavelets (or derivatives/integrals of wavelets) at different scales and translation levels; see, for instance, [25–27] for some indicative references pertaining to calculation of such interaction coefficients. Specifically, in the field of engineering dynamics, Spanos and co-workers developed recently a periodized version of GHWs to address the non-orthogonality of the GHW basis on a finite interval [21]. In this regard, interaction coefficients were derived in closed form and were employed for obtaining an analytical relationship between wavelet coefficients of the system excitation and of the system response. In comparison to alternative earlier efforts towards deriving GHW-based input-output (excitation-response) relationships (e.g., [16, 17]), the approach in [21] circumvented the assumption of local stationarity and yielded a higher degree of accuracy in predicting the system response. The basic aspects of the periodized GHWs and the associated interaction coefficients are elucidated in the following for completeness. The interested reader is also directed to [21] for a more detailed presentation.

A periodized GHW is defined in the time domain as [21]

$$\psi^{\mathrm{G,per}}_{(m_i,n_i),k}(t) = \frac{1}{n-m}\sum_{q=m_i}^{n_i} e^{\mathrm{i}\Delta\omega q\left(t-\frac{kT_0}{n-m}\right)} , \tag{1}$$

where (m_i, n_i) denote the scale indices, i is the subscript for the i-th scale, and $k = 0, 1, \ldots, N_t$, with $N_t = (n-m)-1$, denotes the translation index. A uniform constant bandwidth is chosen for all scales under consideration in the ensuing analysis, i.e., $n_i - m_i = n_j - m_j = n - m$, $i, j = 1, 2, \ldots, N_\Omega$, where $N_\Omega = N/2(n-m)$. Further, $T_0 = N\Delta t$ is the time duration of the discretized signal, where N is the total number of sampling points and $\Delta\omega = 2\pi/T_0$.

The periodized GHW of a continuous function $f(t)$ defined in the interval $[0, T_0]$ is given by [21]

$$W^f_{(m_i,n_i),k} = \frac{n-m}{T_0}\int_0^{T_0} f(t)\bar{\psi}^{\text{G, per}}_{(m_i,n_i),k}(t)\mathrm{d}t = \frac{n-m}{T_0}\left\langle f(t), \bar{\psi}^{\mathrm{G,per}}_{(m_i,n_i),k}(t)\right\rangle_0^{T_0} , \tag{2}$$

where $\langle\cdot\rangle$ represents the inner product over the interval $[0, T_0]$ and the bar over a symbol denotes complex conjugation. Moreover, based on the orthogonality properties of the periodized GHW over a finite time domain, a signal $f(t)$ can be reconstructed as

$$f(t)=\sum_i\sum_k W^f_{(m_i,n_i),k}\psi^{\text{G,per}}_{(m_i,n_i),k}(t)+\sum_i\sum_k \bar{W}^f_{(m_i,n_i),k}\bar{\psi}^{\text{G,per}}_{(m_i,n_i),k}(t). \tag{3}$$

If $f(t)$ is a real valued signal, Eq. (3) becomes

$$f(t)=2\mathrm{Re}\left[\sum_i\sum_k W^f_{(m_i,n_i),k}\psi^{\text{G,per}}_{(m_i,n_i),k}\right], \tag{4}$$

where $\mathrm{Re}[\cdot]$ denotes the real part of the signal.

Further, the periodized GHW interaction coefficients of the zero-, first- and second-order are given by

$$C^0_{i,k,j,l}=\left\langle\psi^{\text{G,per}}_{(m_i,n_i),k}(t),\psi^{\text{G,per}}_{(m_j,n_j),l}(t)\right\rangle_0^{T_0}=\begin{cases}\frac{T_0}{n-m}, & i=j,k=l\\ 0, & \text{otherwise}\end{cases}, \tag{5}$$

$$\begin{aligned}C^1_{i,k,j,l} &= \left\langle\dot{\psi}^{\text{G,per}}_{(m_i,n_i),k}(t),\psi^{\text{G,per}}_{(m_j,n_j),l}(t)\right\rangle_0^{T_0}\\ &= \begin{cases}\frac{\mathrm{i}\pi(n+m)}{n-m}, & i=j,k=l\\ \frac{2\pi\mathrm{i}}{(n-m)^2}\sum\limits_{q=m_i}^{n_i} q e^{\mathrm{i}2\pi q\frac{l-k}{n-m}}, & i=j,k\neq l\\ 0, & \text{otherwise}\end{cases}\end{aligned} \tag{6}$$

and

$$\begin{aligned}C^2_{i,k,j,l} &= \left\langle\ddot{\psi}^{\text{G,per}}_{(m_i,n_i),k}(t),\psi^{\text{G,per}}_{(m_j,n_j),l}(t)\right\rangle_0^{T_0}\\ &= \begin{cases}\frac{-\left(2(n^3-m^3)+3(n^2+m^2)+(n-m)\right)}{3(\pi\Delta\omega)^{-1}(n-m)^2}, & i=j,k=l\\ \frac{-2\pi\Delta\omega}{(n-m)^2}\sum\limits_{q=m_i}^{n_i} q^2 e^{\mathrm{i}2\pi q\frac{l-k}{n-m}}, & i=j,k\neq l\\ 0, & \text{otherwise}\end{cases},\end{aligned} \tag{7}$$

respectively.

Clearly, the importance of the closed form expressions in Eqs. (5)-(7) is paramount for deriving GHW-based input-output (excitation-response) relationships pertaining to second-order (stochastic) differential equations governing the dynamics of diverse engineering systems [21, 23, 28]. In the following section, the stochastic response determination methodology and input-output relationships developed in [21] are generalized to account for singular parameter matrices in the system equations of motion.

2.2. GHW-based input-output (excitation-response) relationships for linear MDOF systems with singular parameter matrices

In this section, the GHW-based excitation-response relationships derived in [21] are generalized to account for MDOF systems exhibiting singular parameter matrices. Specifically, the linear system response EPS matrix is determined by relying on a GHW-based expansion of the response process, by considering the interaction coefficients of Eqs. (5)-(7), and by employing the MP generalized matrix inverse operation.

In this regard, the governing equations of motion of an n_0-DOF linear time-variant system are given by

$$\mathbf{M}_{\mathbf{x}}(t)\ddot{\mathbf{x}}(t) + \mathbf{C}_{\mathbf{x}}(t)\dot{\mathbf{x}}(t) + \mathbf{K}_{\mathbf{x}}(t)\mathbf{x}(t) = \mathbf{Q}_{\mathbf{x}}(t), \tag{8}$$

where $\mathbf{x}$ is the n_0-dimensional response vector; $\mathbf{M}_{\mathbf{x}}(t)$, $\mathbf{C}_{\mathbf{x}}(t)$ and $\mathbf{K}_{\mathbf{x}}(t)$ denote, respectively, the (possibly singular) time-varying mass, damping and stiffness $n_0 \times n_0$ matrices; and $\mathbf{Q}_{\mathbf{x}}(t)$ represents the n_0-dimensional system excitation, which is modeled as a non-stationary zero-mean stochastic process. Next, consider the case that the system is subjected to m_0 linear constraints of the general form [29, 30]

$$\mathbf{A}\ddot{\mathbf{x}}(t) + \mathbf{E}\dot{\mathbf{x}}(t) + \mathbf{L}\mathbf{x}(t) = \mathbf{F}(t), \tag{9}$$

where $\mathbf{A}, \mathbf{E}$ and $\mathbf{L}$ are $m_0 \times n_0$ coefficient matrices and $\mathbf{F}(t)$ is an m_0-dimensional vector. The combined system of Eqs. (8) and (9) is cast in the form

$$\tilde{\mathbf{M}}_{\mathbf{x}}(t)\ddot{\mathbf{x}}(t) + \tilde{\mathbf{C}}_{\mathbf{x}}(t)\dot{\mathbf{x}}(t) + \tilde{\mathbf{K}}_{\mathbf{x}}(t)\mathbf{x}(t) = \tilde{\mathbf{Q}}_{\mathbf{x}}(t), \tag{10}$$

where $\tilde{\mathbf{M}}_{\mathbf{x}}(t), \tilde{\mathbf{C}}_{\mathbf{x}}(t), \tilde{\mathbf{K}}_{\mathbf{x}}(t)$ and $\tilde{\mathbf{Q}}_{\mathbf{x}}(t)$ denote, respectively, the $(n_0 + m_0) \times n_0$ augmented mass, damping and stiffness time-varying matrices given by

$$\tilde{\mathbf{M}}_{\mathbf{x}}(t) = \begin{bmatrix} \mathbf{P}\mathbf{M}_{\mathbf{x}}(t) \\ \mathbf{A} \end{bmatrix}, \quad \tilde{\mathbf{C}}_{\mathbf{x}}(t) = \begin{bmatrix} \mathbf{P}\mathbf{C}_{\mathbf{x}}(t) \\ \mathbf{E} \end{bmatrix}, \quad \tilde{\mathbf{K}}_{\mathbf{x}}(t) = \begin{bmatrix} \mathbf{P}\mathbf{K}_{\mathbf{x}}(t) \\ \mathbf{L} \end{bmatrix} \tag{11}$$

and

$$\tilde{\mathbf{Q}}_{\mathbf{x}}(t) = \begin{bmatrix} \mathbf{P}\mathbf{Q}_{\mathbf{x}}(t) \\ \mathbf{F}(t) \end{bmatrix} \tag{12}$$

is the augmented excitation $(m_0 + n_0)$-dimensional vector. In Eqs. (11) and (12), $\mathbf{P}$ is a $(n_0 + m_0) \times n_0$ matrix interconnecting the constraints to the equations of motion. In fact, for the special case of utilizing a set of dependent/redundant coordinates, it has been shown (e.g., [31–34]) that $\mathbf{P}$ takes the form

$$\mathbf{P} = \mathbf{I} - \mathbf{A}^{+}\mathbf{A}, \tag{13}$$

where "$+$" denotes the MP inverse of a matrix. The interested reader is also directed to [35, 36] for a broader perspective.

Further, considering the expansion of Eq. (4) for the excitation and the response processes, Eq. (10) is cast in the form

$$\begin{aligned}
&\tilde{\mathbf{M}}_{\mathbf{x}}(t) \sum_i \sum_k \left[\mathbf{W}^{\mathbf{x}}_{(m_i,n_i),k} \ddot{\psi}^{\text{G,per}}_{(m_i,n_i),k}(t) + \bar{\mathbf{W}}^{\mathbf{x}}_{(m_i,n_i),k} \ddot{\bar{\psi}}^{\text{G,per}}_{(m_i,n_i),k}(t) \right] \\
&+ \tilde{\mathbf{C}}_{\mathbf{x}}(t) \sum_i \sum_k \left[\mathbf{W}^{\mathbf{x}}_{(m_i,n_i),k} \dot{\psi}^{\text{G,per}}_{(m_i,n_i),k}(t) + \bar{\mathbf{W}}^{\mathbf{x}}_{(m_i,n_i),k} \dot{\bar{\psi}}^{\text{G,per}}_{(m_i,n_i),k}(t) \right] \\
&+ \tilde{\mathbf{K}}_{\mathbf{x}}(t) \sum_i \sum_k \left[\mathbf{W}^{\mathbf{x}}_{(m_i,n_i),k} \psi^{\text{G,per}}_{(m_i,n_i),k}(t) + \bar{\mathbf{W}}^{\mathbf{x}}_{(m_i,n_i),k} \bar{\psi}^{\text{G,per}}_{(m_i,n_i),k}(t) \right] = \\
&\sum_i \sum_k \left[\mathbf{W}^{\tilde{\mathbf{Q}}_{\mathbf{x}}}_{(m_i,n_i),k} \psi^{\text{G,per}}_{(m_i,n_i),k}(t) + \bar{\mathbf{W}}^{\tilde{\mathbf{Q}}_{\mathbf{x}}}_{(m_i,n_i),k} \bar{\psi}^{\text{G,per}}_{(m_i,n_i),k}(t) \right].
\end{aligned} \tag{14}$$

Next, post-multiplying Eq. (14) by $\bar{\psi}^{\text{G,per}}_{(m_j,n_j),l}(t)$, integrating over $[0, T_0]$, taking into account the interaction coefficients in Eq. (5)-(7), and considering the time-variant matrices $\tilde{\mathbf{M}}_{\mathbf{x}}(t)$, $\tilde{\mathbf{C}}_{\mathbf{x}}(t)$ and $\tilde{\mathbf{K}}_{\mathbf{x}}(t)$ as slowly varying, and thus, approximately constant over the compact support of the GHW (i.e., $\tilde{\mathbf{M}}_{\mathbf{x}}(t) \approx \tilde{\mathbf{M}}_{\mathbf{x},k}$, $\tilde{\mathbf{C}}_{\mathbf{x}}(t) \approx \tilde{\mathbf{C}}_{\mathbf{x},k}$ and $\tilde{\mathbf{K}}_{\mathbf{x}}(t) \approx \tilde{\mathbf{K}}_{\mathbf{x},k}$), yields

$$\sum_i \sum_k \mathbf{B}_{i,k,j,l} \mathbf{W}^{\mathbf{x}}_{(m_i,n_i),k} = \frac{T_0}{n-m} \mathbf{W}^{\tilde{\mathbf{Q}}_{\mathbf{x}}}_{(m_j,n_j),l}, \tag{15}$$

where the $(n_0 + m_0) \times n_0$ matrix $\mathbf{B}_{i,k,j,l}$ is given by

$$\mathbf{B}_{i,k,j,l} = C^2_{i,k,j,l} \tilde{\mathbf{M}}_{\mathbf{x},k} + C^1_{i,k,j,l} \tilde{\mathbf{C}}_{\mathbf{x},k} + C^0_{i,k,j,l} \tilde{\mathbf{K}}_{\mathbf{x},k}. \tag{16}$$

Furthermore, noticing that the interaction coefficients defined in Eqs. (5)-(7) are equal to zero for $i \neq j$, and also denoting for simplicity $\mathbf{B}^j_{k,l} = \mathbf{B}_{i,k,j,l}$, Eq. (15) is cast, equivalently, in the form

$$\begin{bmatrix} \sum\limits_k \mathbf{B}^j_{k,1} \mathbf{W}^{\mathbf{x}}_{(m_j,n_j),1} \\ \sum\limits_k \mathbf{B}^j_{k,2} \mathbf{W}^{\mathbf{x}}_{(m_j,n_j),2} \\ \vdots \\ \sum\limits_k \mathbf{B}^j_{k,N_t} \mathbf{W}^{\mathbf{x}}_{(m_j,n_j),k} \end{bmatrix} = \frac{T_0}{n-m} \begin{bmatrix} \mathbf{W}^{\tilde{\mathbf{Q}}_{\mathbf{x}}}_{(m_j,n_j),1} \\ \mathbf{W}^{\tilde{\mathbf{Q}}_{\mathbf{x}}}_{(m_j,n_j),2} \\ \vdots \\ \mathbf{W}^{\tilde{\mathbf{Q}}_{\mathbf{x}}}_{(m_j,n_j),N_t} \end{bmatrix}, \tag{17}$$

for $l = 1, \ldots, N_t$, with $N_t = n - m$. Alternatively, Eq. (17) is written as

$$\mathbf{B}^j \mathbf{W}^j_{\mathbf{x}} = \frac{T_0}{n-m} \mathbf{W}^j_{\tilde{\mathbf{Q}}_{\mathbf{x}}}, \tag{18}$$

where the $(m_0 + n_0)N_t \times (n_0 N_t)$ matrix $\mathbf{B}^j$ is defined as

$$\mathbf{B}^j = \begin{bmatrix} \mathbf{B}^j_{1,1} & \mathbf{B}^j_{2,1} & \cdots & \mathbf{B}^j_{N_t,1} \\ \mathbf{B}^j_{1,2} & \mathbf{B}^j_{2,2} & \ddots & \mathbf{B}^j_{N_t,2} \\ \vdots & \vdots & \vdots & \vdots \\ \mathbf{B}^j_{1,N_t} & \mathbf{B}^j_{2,N_t} & \cdots & \mathbf{B}^j_{N_t,N_t} \end{bmatrix} \tag{19}$$

and the $(n_0 N_t)$- and $(m_o + n_0)N_t$-dimensional vectors $\mathbf{W}^j_{\mathbf{x}}$ and $\mathbf{W}^j_{\tilde{\mathbf{Q}}_{\mathbf{x}}}$ are given by

$$\mathbf{W}^j_{\mathbf{x}} = \begin{bmatrix} \mathbf{W}^{\mathbf{x}}_{(m_j,n_j),1} \\ \mathbf{W}^{\mathbf{x}}_{(m_j,n_j),2} \\ \vdots \\ \mathbf{W}^{\mathbf{x}}_{(m_j,n_j),N_t} \end{bmatrix} \tag{20}$$

and

$$\mathbf{W}^j_{\tilde{\mathbf{Q}}_{\mathbf{x}}} = \begin{bmatrix} \mathbf{W}^{\tilde{\mathbf{Q}}_{\mathbf{x}}}_{(m_j,n_j),1} \\ \mathbf{W}^{\tilde{\mathbf{Q}}_{\mathbf{x}}}_{(m_j,n_j),2} \\ \vdots \\ \mathbf{W}^{\tilde{\mathbf{Q}}_{\mathbf{x}}}_{(m_j,n_j),N_t} \end{bmatrix}, \tag{21}$$

respectively.

Clearly, Eq. (18) represents a GHW-based input-output relationship connecting the wavelet coefficients of the excitation and of the response processes. In passing, note that a similar relationship was derived in [21] restricted, however, to the special case of matrix $\mathbf{B}^j$ being a square, invertible matrix. Herein, due to the modeling of the system governing equations and the definition of the parameter matrices in Eqs. (8)-(10), $\mathbf{B}^j$ can become a singular matrix (see also Eq. (16)). Thus, a special treatment is required for "inverting" $\mathbf{B}^j$ and solving for the response wavelet coefficient matrix $\mathbf{W}_{\mathbf{x}}^j$ to be used in the calculation of the response EPS matrix. In the following, this is done by resorting to the theory of generalized matrix inverses and to the MP matrix inverse operation; see also [33, 34, 37] for some recent indicative papers, and Appendix for more details.

Specifically, considering the MP generalized matrix inverse of $\mathbf{B}^j$, Eq. (17) yields (see Appendix)

$$\mathbf{W}_{\mathbf{x}}^j = \frac{T_0}{n-m}(\mathbf{B}^j)^+\mathbf{W}_{\tilde{\mathbf{Q}}_{\mathbf{x}}}^j + (\mathbf{I}_{n_0\times n_0} - (\mathbf{B}^j)^+(\mathbf{B}^j))\mathbf{y}_{n_0}, \tag{22}$$

where $\mathbf{y}_{n_0}$ is an arbitrary n_0-dimensional vector. It is readily seen that Eq. (22) defines a family of solutions for the response wavelet coefficients. Nevertheless, for the special case of matrix $\mathbf{B}^j$ being full rank, i.e., rank$(\mathbf{B}^j) = n_0 N_t$, its MP matrix inverse is determined, uniquely, in the form [38, 39]

$$(\mathbf{B}^j)^+ = \left(\left(\overline{\mathbf{B}^j}\right)^{\mathrm{T}}\mathbf{B}^j\right)^{-1}\left(\overline{\mathbf{B}^j}\right)^{\mathrm{T}}. \tag{23}$$

Substituting Eq. (23) into the second term of the right hand-side of Eq. (22) yields

$$\left(\mathbf{I}_{n_0\times n_0} - (\mathbf{B}^j)^+(\mathbf{B}^j)\right)\mathbf{y}_{n_0} = \mathbf{0}, \tag{24}$$

and thus, Eq. (22) simplifies to

$$\mathbf{W}_{\mathbf{x}}^j = \frac{T_0}{n-m}(\mathbf{B}^j)^+\mathbf{W}_{\tilde{\mathbf{Q}}_{\mathbf{x}}}^j. \tag{25}$$

Obviously, Eq. (25) can be construed as a generalization of the input-output relationship derived in [21] to account for systems with singular parameter matrices in a straightforward manner. Indeed, as shown in the numerical examples in section 3, the herein developed technique can address diverse system modeling yielding singular matrices, including structural systems modeled by a set of dependent coordinates, energy harvesters with coupled electromechanical equations, and oscillators subject to stochastic excitations modeled via additional auxiliary state equations.

Further, the problem of estimating the system response EPS based on the wavelet coefficients corresponding to an ensemble of realizations is addressed. In this regard, employing Eq. (25), multiplying both sides with their Hermitian transposes and taking expectation, yields

$$\mathbb{E}\Big[\mathbf{W}^j_{\mathbf{x}}(\mathbf{W}^j_{\mathbf{x}})^{\mathrm{T}}\Big] = \Big(\frac{T_0}{n-m}\Big)^2(\mathbf{B}^j)^+\mathbb{E}\Big[\mathbf{W}^j_{\tilde{\mathbf{Q}}_{\mathbf{x}}}\big(\mathbf{W}^j_{\tilde{\mathbf{Q}}_{\mathbf{x}}}\big)^{\mathrm{T}}\Big]\big((\mathbf{B}^j)^+\big)^{\mathrm{T}}. \tag{26}$$

It is readily seen that based on the formula

$$S_x(\omega_j, t_k) = \frac{T_0}{2\pi(n-m)}\mathbb{E}\Big[\,\big|W^x_{j,k}\big|^2\,\Big], \tag{27}$$

derived in [13, 16], the diagonal terms in Eq. (26) represent response EPS values corresponding to translation levels $k = 1, 2, \ldots, N_t$. Note that additional information (e.g., regarding the phase of the process) is available as well via the off-diagonal elements that provide a measure of the interaction between wavelet coefficients at different time intervals (for a specific scale j). It can be argued that the matrix $\mathbb{E}\Big[\mathbf{W}^j_{\mathbf{x}}\big(\mathbf{W}^j_{\mathbf{x}}\big)^{\mathrm{T}}\Big]$ in Eq. (26) can be construed as a form of "autocorrelation" matrix in the wavelet domain; see also [21] for a relevant discussion.

3. Diverse numerical examples

In this section, various diverse numerical examples are considered for demonstrating the reliability of the herein derived input-output relationship of Eq. (26), which can be construed as a generalization of the methodology developed in [21] to account for singular matrices. These examples pertain to energy harvesters with coupled electromechanical equations, oscillators subject to non-white excitations modeled via additional filter equations, and structural systems modeled by a set of dependent coordinates. It is remarked that the results obtained by the analytical technique require approximately 2-3 s of computation time for the considered examples. These are compared with MCS-based estimates (500 realizations) that require approximately 2-3 min of computation time on the same computer, i.e., a MacBook Pro 2018 laptop with a 2.9 GHz 6-Core Intel Core i9 processor and 16 GB RAM.

3.1. A class of electromechanical energy harvesting systems

A cantilever beam with piezoelectric patches attached near its clamped ends has been one of the most popular and widely studied electromechanical energy harvesters (e.g., [40–42]). Following the presentation and detailed discussion in [40], the dynamics of such a system can be approximated by the following general mathematical model of coupled electromechanical equations, expressed in a non-dimensional form as

$$\ddot{q} + 2\zeta\dot{q} + \frac{\mathrm{d}U(q)}{\mathrm{d}q} + \kappa^2 \upsilon = f(t) \tag{28}$$

$$\dot{\upsilon} + \alpha\upsilon - \dot{q} = 0 \tag{29}$$

where q denotes the response displacement and υ represents the induced voltage in capacitive harvesters or the induced current in inductive ones. Further, ζ is the damping, κ is the coupling coefficient, α is defined as the ratio between the mechanical and electrical time constants of the harvester (see [40]), and $U(q)$ denotes the potential function. Its derivative $\frac{\mathrm{d}U(q)}{\mathrm{d}q}$ represents the restoring force, which is modeled in the ensuing analysis as linear, i.e., $\frac{\mathrm{d}U(q)}{\mathrm{d}q} = q$; see also [41, 42] for alternative nonlinear modeling.

In the following, the excitation $f(t)$ is modeled as a non-stationary stochastic process compatible with the EPS

$$S_f(\omega, t) = d(t)^2 S_0, \tag{30}$$

where S_0 denotes the Gaussian white noise constant power spectrum value, and $d(t)$ represents a time-modulating function. Indicatively, Eq. (30) can describe approximately the relatively slow variations in time of the intensity of the white noise process, and in this regard, $d(t)$ is given by

$$d(t) = 1 + 0.5\cos(\omega_0 t), \tag{31}$$

where $\omega_0 = 0.25\ rad/s$. Further, the parameter values considered herein are $\zeta = 0.1,\ \kappa = 3.25$, $\alpha = 0.8$ and $S_0 = 0.05$.

Although there exist alternative solution treatments in the literature for addressing Eqs. (28) and (29), and for determining relevant response statistics (e.g., [41–43]), the herein developed methodology is employed next for determining the response EPS and for demonstrating that singular matrices can be treated in a straightforward and direct manner.

Specifically, similarly to [41, 42] where the stochastic response analysis of Eqs. (28) and (29) was performed based on a Wiener path integral solution treatment, Eq. (28) can be construed as the governing stochastic differential equation constrained by Eq. (29); see also [44]. In this regard, setting $\mathbf{x}^{\mathrm{T}} = \begin{bmatrix} q & \upsilon \end{bmatrix}$, and differentiating Eq. (29) once with respect to time, the parameter matrices of the constraint Eq. (9) become

$$\mathbf{A} = \begin{bmatrix} -1 & 1 \end{bmatrix}, \ \mathbf{E} = \begin{bmatrix} 0 & \alpha \end{bmatrix}, \ \mathbf{L} = \begin{bmatrix} 0 & 0 \end{bmatrix}, \ F = 0, \tag{32}$$

whereas the matrix $\mathbf{P}$ of Eq. (13) takes the form

$$\mathbf{P} = \begin{bmatrix} 0.5 & 0.5 \\ 0.5 & 0.5 \end{bmatrix}. \tag{33}$$

Further, the parameter matrices in Eq. (11) become

$$\tilde{\mathbf{M}}_{\mathbf{x}} = \begin{bmatrix} 0.5 & 0 \\ 0.5 & 0 \\ -1 & 1 \end{bmatrix}, \ \tilde{\mathbf{C}}_{\mathbf{x}} = \begin{bmatrix} -0.40 & 0.5 \\ -0.40 & 0.5 \\ 0 & 0.8 \end{bmatrix}, \ \tilde{\mathbf{K}}_{\mathbf{x}} = \begin{bmatrix} 0.5 & 5.6812 \\ 0.5 & 5.6813 \\ 0 & 0 \end{bmatrix} \tag{34}$$

and Eq. (12) takes the form

$$\tilde{\mathbf{Q}}_{\mathbf{x}} = \begin{bmatrix} 0.5 \\ 0.5 \\ 0 \end{bmatrix} f(t). \tag{35}$$

Therefore, the excitation EPS matrix corresponding to Eq. (35) becomes

$$\mathbf{S}^{j}_{\tilde{\mathbf{Q}}_{\mathbf{x}}} = \frac{T_0}{2\pi(n-m)} \begin{bmatrix} \mathbf{S}^{j}_{\tilde{\mathbf{Q}}_{\mathbf{x}},(1,1)} & 0 & \cdots & 0 \\ 0 & \mathbf{S}^{j}_{\tilde{\mathbf{Q}}_{\mathbf{x}},(2,2)} & \cdots & 0 \\ \vdots & \vdots & \ddots & \vdots \\ 0 & 0 & \cdots & \mathbf{S}^{j}_{\tilde{\mathbf{Q}}_{\mathbf{x}},(N_t,N_t)} \end{bmatrix}, \tag{36}$$

where

$$\mathbf{S}^{j}_{\tilde{\mathbf{Q}}_{\mathbf{x}},(k,k)} = \begin{bmatrix} 0.25\, d_l^4\, S^{j}_{f,(k,k)} & 0.25\, d_l^4\, S_{f,(k,k)} & 0 \\ 0.25\, d_l^4\, S_{f,(k,k)} & 0.25\, d_l^4\, S_{f,(k,k)} & 0 \\ 0 & 0 & 0 \end{bmatrix}, \tag{37}$$

for $0 \leq k \leq N_t$, and is utilized next for defining $\mathbb{E}\left[\mathbf{W}^j_{\tilde{\mathbf{Q}}_{\mathbf{x}}}\left(\mathbf{W}^j_{\tilde{\mathbf{Q}}_{\mathbf{x}}}\right)^{\mathrm{T}}\right]$ on the right hand-side of Eq. (26). Also, utilizing the parameter matrices in Eq. (34), the matrix $\mathbf{B}^j$ in Eq. (19) is formed for each wavelet band $j = 1, 2, \ldots, 256$ and each time instant to be used in Eq. (26). In fact, it is noted that $\mathbf{B}^j$ has full rank, and thus, Eqs. (25) and (26) can be applied yielding a unique solution for the interaction coefficients of the system response.

In Fig. 1(a), the response EPS for the voltage υ is plotted based on Eqs. (26) and (27), whereas in Fig. 1(b) the response EPS for υ is estimated based on MCS data. Specifically, first, 500 excitation time histories compatible with the EPS in Eq. (30) are generated by the spectral representation method [45] with a signal duration $T_0 = 20.46\ s$, and a cut-off frequency equal to $\omega_u = 50\pi\ rad/s$. Second, the coupled system defined by Eqs. (28) and (29) is solved by resorting to a standard 4^{th} order Runge-Kutta numerical integration scheme, and the response voltage EPS is estimated by utilizing Eq. (27) and using a constant frequency band $n - m = 4$. In Fig. 1(c), comparisons are provided between the MCS-based results and the estimates based on the herein developed methodology for two indicative time instants, i.e., $t = 4\ s$ and $t = 10\ s$. It is readily seen that the herein derived input-output relationship of Eq. (26), which accounts for singular matrices, exhibits a relatively high degree of accuracy in determining the system response EPS.

3.2. Non-white stochastic excitation modeling via auxiliary filter equations

In the field of stochastic engineering dynamics, a non-white excitation process is typically represented in the time domain as the output of a filter subject to white noise (e.g., [36, 46, 47]). In this regard, the state-variable vector is augmented to account for the additional filter equation associated with the non-white excitation. In many cases, the form of the filter equation leads to a system of governing equations with singular parameter matrices. For example, consider a single-DOF linear oscillator of the form

$$m\ddot{q} + c\dot{q} + kq = h(t), \tag{38}$$

where m, c, k are the mass, damping and stiffness parameters of the system and $h(t)$ denotes the excitation, given by

$$h(t) = g(t)y(t). \tag{39}$$

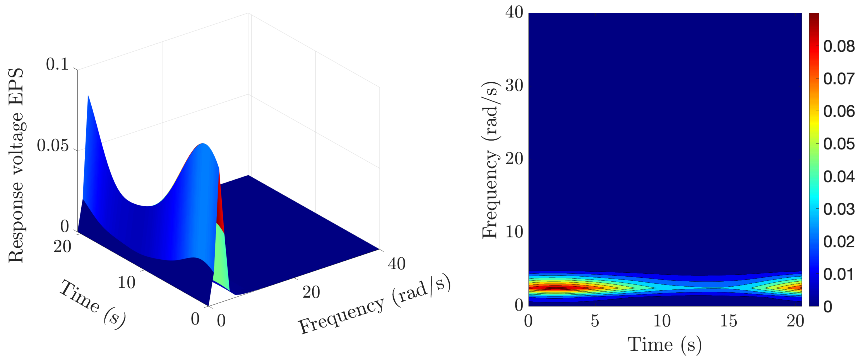

(a)

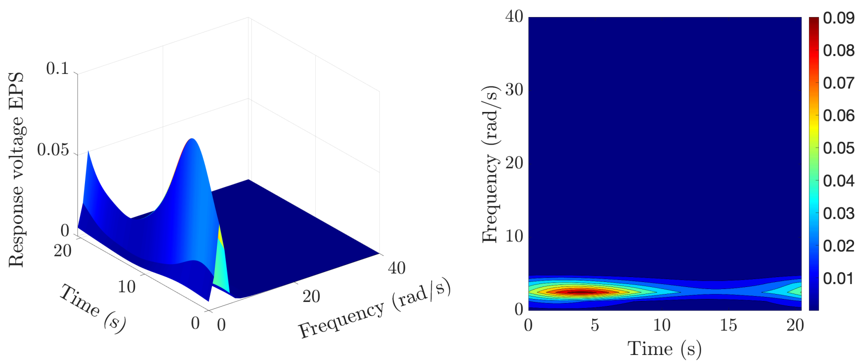

(b)

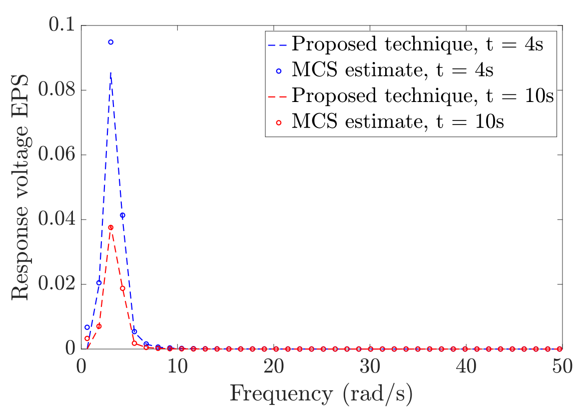

(c)

Fig. 1: Response voltage EPS estimate pertaining to the energy harvesting system of Eqs. (28) and (29) subject to time-modulated Gaussian white noise excitation: (a) Analytical closed-form input-output relationship of Eq. (26), (b) MCS-based estimate (500 realizations), (c) Comparison for two indicative time-instants.

In Eq. (39), $g(t)$ denotes a modulating function of the form [16]

$$g(t) = \lambda(e^{-\alpha t} - e^{-\beta t}), \tag{40}$$

where α, β and λ are parameters controlling the shape of the modulating function. Further, the power spectrum of the stochastic process $y(t)$ is given by

$$S_y(\omega) = \frac{S_0}{c_n^2\omega^2 + k_n^2} \tag{41}$$

which is expressed in the time domain as the output of the first order linear filter

$$c_n\dot{y} + k_n y = w(t). \tag{42}$$

In Eq. (42), $w(t)$ is a Gaussian white noise stochastic process with $\mathbb{E}[w(t)w(t+\tau)] = 2\pi S_0\delta(\tau)$, $\delta(\tau)$ is the Dirac delta function and c_n, k_n are filter parameters.

Next, considering the state vector $\mathbf{x}^{\mathrm{T}} = \begin{bmatrix} q & y & f(t) \end{bmatrix}$, where $f(t) = w(t)$, and taking into account Eqs. (38) and (42), the governing equations take the form of Eq. (8) with

$$\mathbf{M_x} = \begin{bmatrix} m & 0 & 0 \\ 0 & 0 & 0 \\ 0 & 0 & 0 \end{bmatrix}, \; \mathbf{C_x} = \begin{bmatrix} c & 0 & 0 \\ 0 & c_n & 0 \\ 0 & 0 & 0 \end{bmatrix}, \; \mathbf{K_x} = \begin{bmatrix} k & -g(t) & 0 \\ 0 & k_n & -1 \\ 0 & 0 & 1 \end{bmatrix} \tag{43}$$

and

$$\mathbf{Q_x}(t) = \begin{bmatrix} 0 \\ 0 \\ w(t) \end{bmatrix}, \tag{44}$$

whereas the constraint equation parameter matrices corresponding to Eq. (9) become

$$\mathbf{A} = \begin{bmatrix} 0 & c_n & 0 \end{bmatrix}, \; \mathbf{E} = \begin{bmatrix} 0 & k_n & 1 \end{bmatrix}, \; \mathbf{L} = \mathbf{0}, \; F = 0. \tag{45}$$

Therefore, the matrix $\mathbf{P}$ of Eq. (13) is given by

$$\mathbf{P} = \begin{bmatrix} c_n & 0 & 0 \\ 0 & 0 & 0 \\ 0 & 0 & c_n \end{bmatrix}. \tag{46}$$

Note that the system defined in Eq. (43) is time-variant, since the matrix $\mathbf{K_x}$ contains the function $g(t)$. Nevertheless, this poses no difficulty in applying the proposed methodology since it can readily treat time-variant parameter matrices as shown in Eq. (8). Further, the matrices of Eq. (10) for the herein considered system take the form

$$\tilde{\mathbf{M}}_{\mathbf{x}} = \begin{bmatrix} m & 0 & 0 \\ 0 & 0 & 0 \\ 0 & 0 & 0 \\ 0 & c_n & 0 \end{bmatrix}, \ \tilde{\mathbf{C}}_{\mathbf{x}} = \begin{bmatrix} c & 0 & 0 \\ 0 & 0 & 0 \\ 0 & 0 & 0 \\ 0 & k_n & 1 \end{bmatrix}, \ \tilde{\mathbf{K}}_{\mathbf{x}} = \begin{bmatrix} k & -g(t) & 0 \\ 0 & 0 & 0 \\ 0 & 0 & 1 \\ 0 & 0 & 0 \end{bmatrix} \tag{47}$$

and

$$\tilde{\mathbf{Q}}_{\mathbf{x}} = \begin{bmatrix} 0 \\ 0 \\ 1 \\ 0 \end{bmatrix} w(t). \tag{48}$$

Therefore, the excitation EPS matrix corresponding to Eq. (48) is written in the form of Eq. (36), where

$$\mathbf{S}^{j}_{\tilde{\mathbf{Q}}_{\mathbf{x}},(k,k)} = \begin{bmatrix} 0 & 0 & 0 & 0 \\ 0 & 0 & 0 & 0 \\ 0 & 0 & S_{w,(k,k)} & 0 \\ 0 & 0 & 0 & 0 \end{bmatrix}, \tag{49}$$

for $0 \leq k \leq N_t$, and is utilized next for defining $\mathbb{E}\left[\mathbf{W}^{j}_{\tilde{\mathbf{Q}}_{\mathbf{x}}} \left(\mathbf{W}^{j}_{\tilde{\mathbf{Q}}_{\mathbf{x}}}\right)^{\mathrm{T}}\right]$ on the right hand-side of Eq. (26). The parameter values considered herein are $m_1 = 1\ kg/(ms^2)$, $c_1 = 4.3\ Ns/m$, $k_1 = 256\ N/m$, $k_n = 8\ N/m$, $c_n = 1\ Ns/m$ and $S_0 = 1$. The resulting $\mathbf{B}^j$ has full rank, and thus, the simplified expression in Eq. (23) is used for computing the MP matrix inverse. This yields a unique solution for the interaction coefficients of the system response, which is determined by Eq. (26). The obtained response displacement EPS is shown in Fig. 2(a), whereas in Fig. 2(b) the response EPS is determined based on MCS data generated by solving numerically Eq. (38) via a Runge-Kutta integration scheme in conjunction with the spectral representation methodology [45] for generating excitation realizations. Note that the discrepancies observed in Figs. 2(a) and 2(b) near the ends of the time domain are attributed to “end effects” due to the application of the wavelet transform. The interested reader is directed to [48] for more details and possible melioration treatments such as zero-padding. Further, the analytical solution and MCS-based estimate are compared in Fig. 2(c) for two indicative time instants, i.e., $t = 4\ s$ and $t = 7\ s$. Clearly, the results obtained by the herein proposed input-output relationship of Eq. (26) for determining the response EPS of systems exhibiting singular matrices are in good agreement with the corresponding MCS estimates.

3.3. Structural systems modeled via dependent coordinates

It is common practice in the field of engineering dynamics to utilize the minimum number of coordinates (generalized coordinates) for formulating the system equations of motion (e.g., [46]). In general, this yields not only non-singular, but also positive definite parameter matrices in the governing equations. Nevertheless, it has been argued recently that the explicit formulation of the equations of motion based on generalized coordinates can be a cumbersome task, and thus, alternative approaches have been proposed based, indicatively, on utilizing a set of dependent/redundant DOFs in conjunction with a number of constraint equations (e.g., [29, 49, 50]). Although this unconventional modeling appears to be advantageous from a computational efficiency perspective [51], it leads to equations of the form of Eq. (10) exhibiting singular matrices.

In this section, the herein developed solution methodology based on periodized GHWs is employed for determining the response EPS of a stochastically excited structural system modeled via dependent coordinates. Specifically, the 2-DOF system of Fig. 3 is considered, where mass m_1 is connected to the foundation via a spring and a damper with coefficients k_1 and c_1, respectively. Further, it is connected to mass m_2 via a spring and a damper with coefficients k_2 and c_2, respectively. The applied excitation stochastic processes $Q_1(t)$ and $Q_2(t)$ are compatible with an EPS given by

$$S_f(\omega, t) = S_0 \left(\frac{\omega t}{5\pi}\right)^2 \exp(-c_0 t) t^2 \exp\left(-\left(\frac{\omega}{5\pi}\right)^2 t\right). \tag{50}$$

It can be argued that the EPS form in Eq. (50) comprises some of the main characteristics of earthquake excitations, such as decreasing of the dominant frequency with time (e.g., [52, 53]). The parameter values considered in the ensuing analysis are: $m_i = 1\ kg/(ms^2)$, $c_i = 4.3\ Ns/m$, $k_i = 256\ N/m$, for $i = 1, 2$, and $S_0 = 1\ m^2/s^3$, $c_0 = 0.15$. The system excitation is applied for time $[0, T_0]$, with $T_0 = 20.48\ s$, considering $N_t = 1024$ points and cut-off frequency equal to $10\pi\ rad/s$. Also, a constant bandwidth resolution of $n - m = 4$ is used.

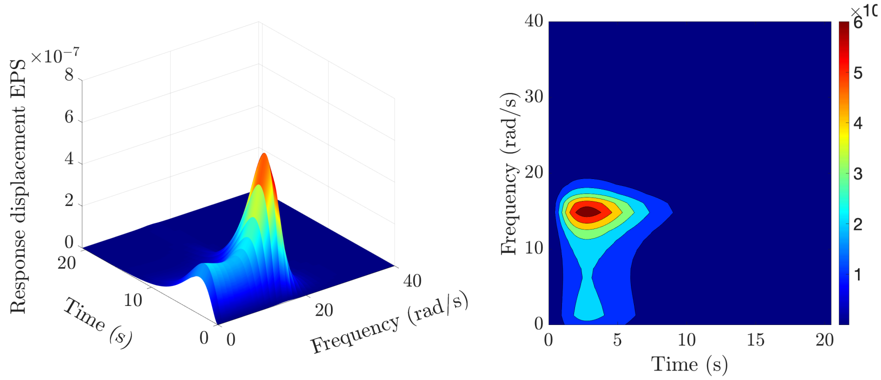

(a)

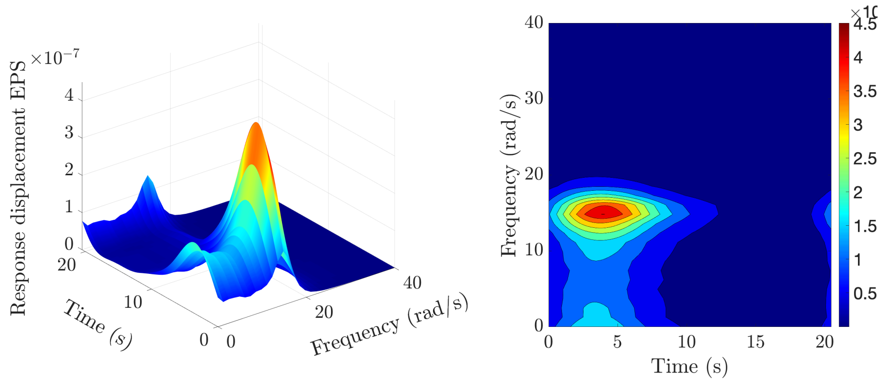

(b)

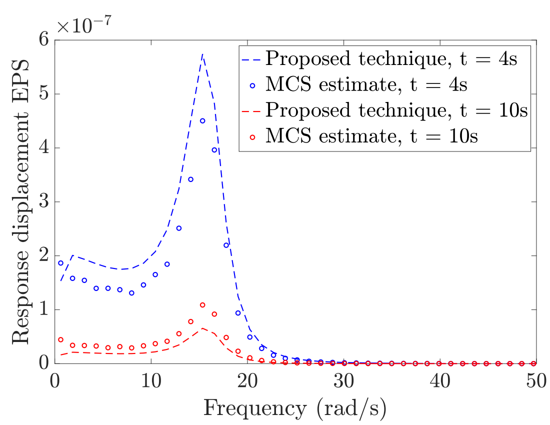

(c)

Fig. 2: Response displacement EPS pertaining to the oscillator in Eq. (38) subject to a time-modulated non-stationary excitation: (a) Analytical closed-form input-output relationship of Eq. (26), (b) MCS-based estimate (500 realizations), (c) Comparison for two indicative time instants.

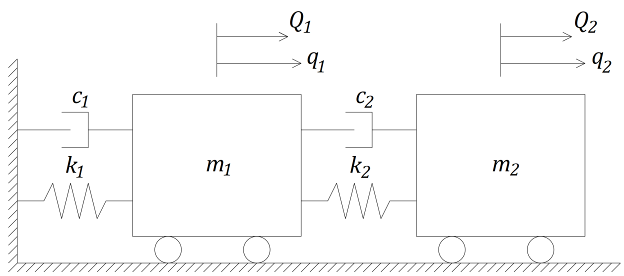

Fig. 3: Two-degree-of-freedom linear structural system subjected to non-stationary stochastic excitation.

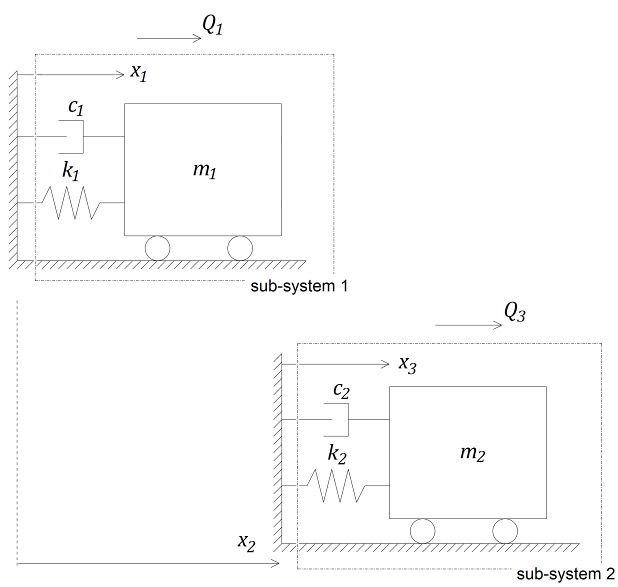

Fig. 4: Modeling the system in Fig. 3 by using dependent coordinates.

Next, utilizing the generalized coordinates vector $\mathbf{q}^{\mathrm{T}} = \begin{bmatrix} q_1 & q_2 \end{bmatrix}$, the governing equations of motion become

$$m_1\ddot{q}_1 + (c_1 + c_2)\dot{q}_1 + (k_1 + k_2)q_1 - c_2\dot{q}_2 - k_2 q_2 = -m_1 Q_1(t), \tag{51}$$

$$m_2\ddot{q}_2 - c_2\dot{q}_1 - k_2 q_1 + c_2\dot{q}_2 + k_2 q_2 = -m_2 Q_2(t). \tag{52}$$

Further, adopting a dependent coordinates modeling for the derivation of the equations of motion (see Fig. 4), the coordinates vector $\mathbf{x}^{\mathrm{T}} = \begin{bmatrix} x_1 & x_2 & x_3 \end{bmatrix}$ is considered in conjunction with the constraint equation

$$x_2 = x_1 + d, \tag{53}$$

where d denotes the physical length of mass m_1. In this regard, the parameter matrices corresponding to Eq. (8) take the form

$$\mathbf{M_x} = \begin{bmatrix} 1 & 0 & 0 \\ 0 & 1 & 1 \\ 0 & 1 & 1 \end{bmatrix}, \; \mathbf{C_x} = \begin{bmatrix} 4.3 & 0 & 0 \\ 0 & 0 & 0 \\ 0 & 0 & 4.3 \end{bmatrix}, \; \mathbf{K_x} = \begin{bmatrix} 256 & 0 & 0 \\ 0 & 0 & 0 \\ 0 & 0 & 256 \end{bmatrix} \tag{54}$$

and

$$\mathbf{Q_x} = \begin{bmatrix} Q_1 \\ Q_3 \\ Q_3 \end{bmatrix}, \tag{55}$$

whereas twice differentiating the constraint Eq. (53), the matrices in Eq. (9) take the form

$$\mathbf{A} = \begin{bmatrix} 1 & -1 & 0 \end{bmatrix}, \; \mathbf{E} = \mathbf{L} = \mathbf{0}_{1\times 3}, \; F = 0. \tag{56}$$

Also, the matrix $\mathbf{P}$ in Eq. (13) is given by

$$\mathbf{P} = \begin{bmatrix} 0.5 & 0.5 & 0 \\ 0.5 & 0.5 & 0 \\ 0 & 0 & 1 \end{bmatrix}, \tag{57}$$

and thus, the matrices in Eqs. (11) and (12) become

$$\tilde{\mathbf{M}}_{\mathbf{x}} = \begin{bmatrix} 0.5 & 0.5 & 0.5 \\ 0.5 & 0.5 & 0.5 \\ 0 & 1 & 1 \\ 1 & -1 & 0 \end{bmatrix}, \tilde{\mathbf{C}}_{\mathbf{x}} = \begin{bmatrix} 2.15 & 0 & 0 \\ 2.15 & 0 & 0 \\ 0 & 0 & 4.3 \\ 0 & 0 & 0 \end{bmatrix}, \tilde{\mathbf{K}}_{\mathbf{x}} = \begin{bmatrix} 128 & 0 & 0 \\ 128 & 0 & 0 \\ 0 & 0 & 256 \\ 0 & 0 & 0 \end{bmatrix} \tag{58}$$

and

$$\tilde{\mathbf{Q}}_{\mathbf{x}} = \begin{bmatrix} Q_1 \\ Q_3 \\ Q_3 \\ 0 \end{bmatrix}. \tag{59}$$

Accordingly, the excitation EPS matrix corresponding to Eq. (59) is written as in Eq. (36), where

$$\mathbf{S}^j_{\tilde{\mathbf{Q}}_{\mathbf{x}},(k,k)} = \begin{bmatrix} S^j_{f,(k,k)} & 0 & 0 & 0 \\ 0 & S^j_{f,(k,k)} & S^j_{f,(k,k)} & 0 \\ 0 & S^j_{f,(k,k)} & S^j_{f,(k,k)} & 0 \\ 0 & 0 & 0 & 0 \end{bmatrix}, \tag{60}$$

for $0 \leq k \leq N_t$, and is utilized next for defining $\mathbb{E}\left[\mathbf{W}^j_{\tilde{\mathbf{Q}}_{\mathbf{x}}}\left(\mathbf{W}^j_{\tilde{\mathbf{Q}}_{\mathbf{x}}}\right)^{\mathrm{T}}\right]$ on the right hand-side of Eq. (26). The matrix $\mathbf{B}^j$ in Eq. (19) is constructed for each wavelet band $j = 1, 2, \ldots, 128$, and each time instant, and since it has full rank, its MP inverse is given by Eq. (23). Next, the response displacement EPS is determined by utilizing Eq. (26). The analytical results pertaining to the 1^{st} and 3^{rd} DOF of the system in Fig. 4 are shown in Figs. 5(a) and 6(a), respectively.

Further, the technique is also applied to the system of Eqs. (51-52), which is modeled based on generalized (independent) coordinates. Clearly, based on Figs. (3-4), $q_1 = x_1$ and $q_2 - q_1 = x_3$. In this regard, $\mathbf{B}^j$ in the resulting Eq. (18) is a square invertible matrix, and thus, Eq. (18) can be readily solved for the response wavelet coefficients $\mathbf{W}^j_{\mathbf{q}}$ to be used for determining the response power spectra via Eqs. (26-27). In fact, the computed power spectra $S_{q_1}(\omega, t)$ and $S_{q_2-q_1}(\omega, t)$ are plotted in Figs. 5(b) and 6(b), respectively. As anticipated due to the relationships $q_1 = x_1$ and $q_2 - q_1 = x_3$, note that $S_{x_1}(\omega, t)$ in Fig. 5(a) and $S_{x_3}(\omega, t)$ in Fig. 6(a) are identical to $S_{q_1}(\omega, t)$ and $S_{q_2-q_1}(\omega, t)$, respectively.

Overall, it is seen that the solution obtained by the herein developed technique accounting for dependent coordinates and singular matrices is identical to the solution determined based on an alternative system modeling employing generalized (independent) coordinates and featuring square, invertible, matrices. In other words, the herein proposed solution treatment of a system with singular matrices does not introduce any additional approximations compared to treating an equivalent system with square invertible matrices.

Also, note that, for cases of square invertible matrices, the technique can be construed as an extension of the standard periodized GHW technique in [21] to treat MDOF systems. Furthermore, MCS-based EPS estimates (500 realizations) are also included in Figs. 5(c) and 6(c), whereas response EPS estimates at two indicative time instants are plotted in Fig. 7. Comparisons indicate a satisfactory degree of accuracy exhibited by the periodized GHW technique.

4. Concluding remarks

In this paper, a technique based on periodized GHWs has been developed for joint time-frequency response analysis of linear systems with singular parameter matrices. This has been done by resorting to concepts and tools related to the MP generalized matrix inverse theory. Specifically, considering GHW-based expansions for the excitation and response processes of the system, novel input-output relationships have been derived in the wavelet domain. These have been used for determining the EPS matrix of the system response.

The developed technique can be construed as a generalization of earlier efforts in the literature to account for singular parameter matrices in the governing equations of motion, while its reliability has been demonstrated by comparing the analytical results with pertinent MCS data. This has been done in conjunction with various diverse numerical examples pertaining to energy harvesters with coupled electromechanical equations, oscillators subject to non-white excitations modeled via auxiliary filter equations, and structural systems modeled by a set of dependent coordinates.

Note in passing that the MP matrix inverse operation involves the solution of an optimization problem based on L_2-norm minimization. In this regard, exploring the potential of alternative optimization schemes based, for instance, on L_p-norm ($0 < p < 1$) minimization is identified as future work (e.g., [3, 54]).

Acknowledgement

The authors gratefully acknowledge the support from the European Union's Horizon 2020 research and innovation programme under the Marie Skłodowska-Curie grant agreement No 764547, and from the German Research Foundation under Grant No. FR 4442/2-1.

Appendix

Consider a linear system of equations in the form

$$\mathbf{A}\mathbf{x} = \mathbf{b}, \tag{61}$$

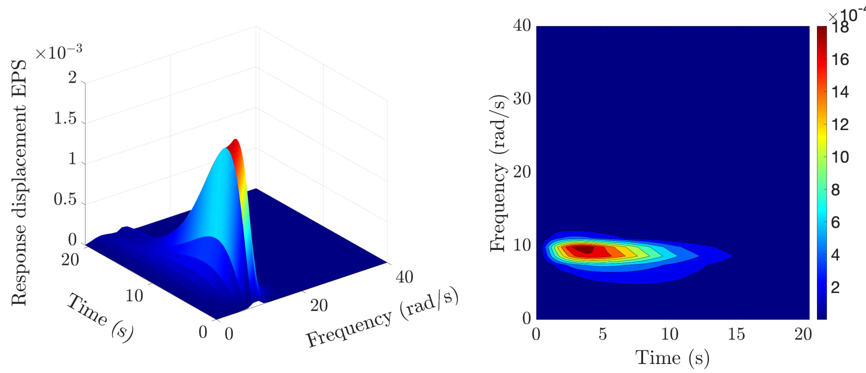

(a)

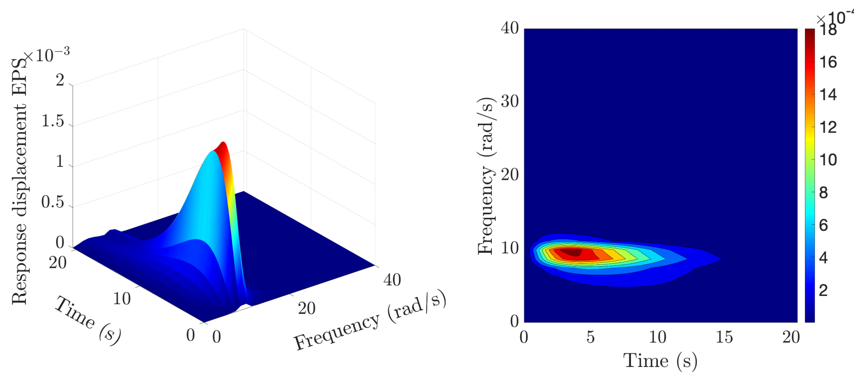

(b)

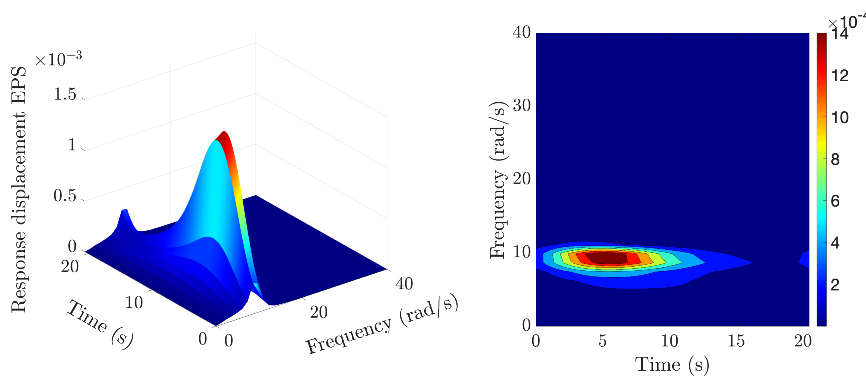

(c)

Fig. 5: Response EPS of a 2-DOF linear system subject to non-stationary stochastic excitation described by the non-separable EPS in Eq. (50): (a) EPS for displacement x_1 based on Eq. (26) with a singular $\mathbf{B}^j$ matrix (dependent coordinates), (b) EPS for displacement q_1 based on Eq. (26) with a square invertible $\mathbf{B}^j$ matrix (generalized coordinates), (c) MCS-based estimate (500 realizations).

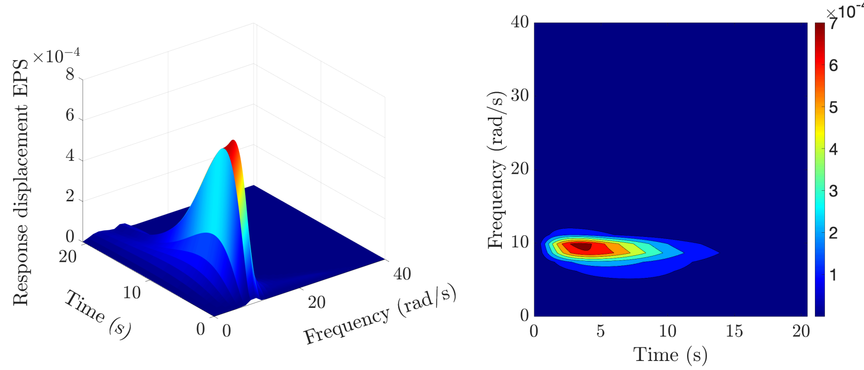

(a)

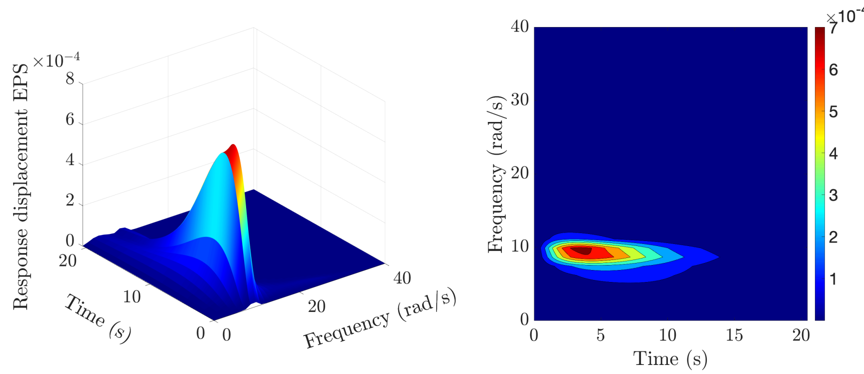

(b)

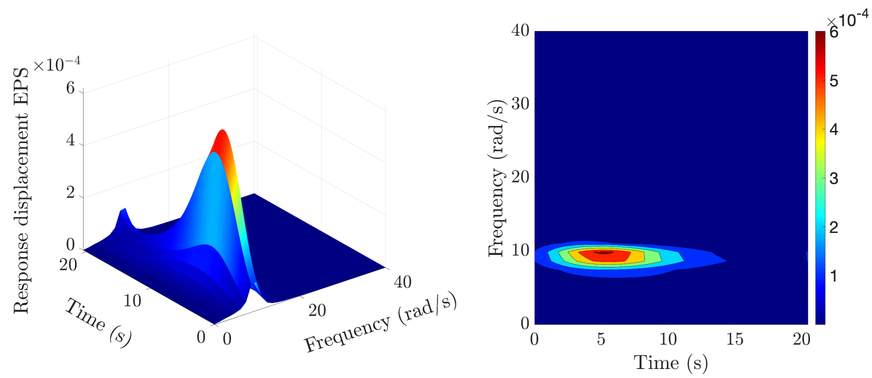

(c)

Fig. 6: Response EPS of a 2-DOF linear system subject to non-stationary stochastic excitation described by the non-separable EPS in Eq. (50): (a) EPS for displacement x_3 based on Eq. (26) with a singular $\mathbf{B}^j$ matrix (dependent coordinates), (b) EPS for displacement $q_2 - q_1$ based on Eq. (26) with a square invertible $\mathbf{B}^j$ matrix (generalized coordinates), (c) MCS-based estimate (500 realizations).

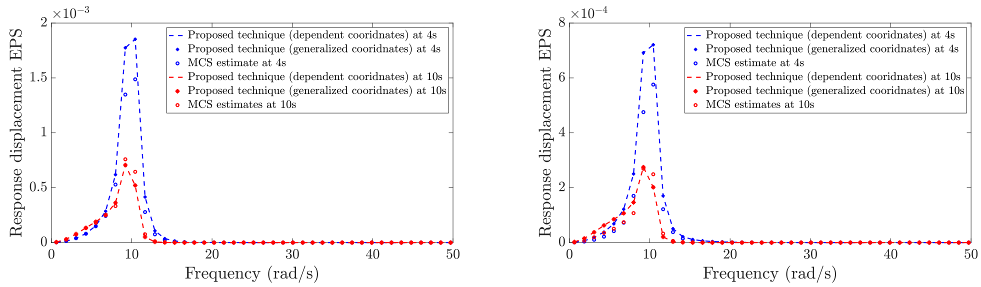

(a) (b)

Fig. 7: Response EPS of a 2-DOF linear system subject to non-stationary stochastic excitation described by the non-separable EPS in Eq. (50) for two indicative time instants: (a) comparisons between analytically determined EPS for x_1, q_1, and MCS estimates (500 realizations), and (b) comparisons between analytically determined EPS for x_2, $q_2 - q_1$, and MCS estimate (500 realizations).

where $\mathbf{A}$ is either a rectangular $m \times n$, or a square but singular $n \times n$ matrix, and x, b are n-dimensional vectors. It is readily seen that solving Eq. (61) necessitates the generalization of the concept of matrix inverse, which has given birth to the theory of generalized matrix inverses [39]. In particular, the Moore-Penrose (MP) generalized matrix inverse is utilized throughout the paper.

Definition. For any matrix $\mathbf{A} \in \mathbb{C}^{m\times n}$, there is a unique matrix $\mathbf{A}^{+} \in \mathbb{C}^{n\times m}$ such that:

$$\mathbf{A}\mathbf{A}^{+}\mathbf{A} = \mathbf{A}, \quad \mathbf{A}^{+}\mathbf{A}\mathbf{A}^{+} = \mathbf{A}^{+}, \quad \overline{\mathbf{A}\mathbf{A}^{+}} = \mathbf{A}\mathbf{A}^{+}, \quad \overline{\mathbf{A}^{+}\mathbf{A}} = \mathbf{A}^{+}\mathbf{A}. \tag{62}$$

The matrix $\mathbf{A}^{+}$ of the Definition is called the MP inverse of $\mathbf{A}$. If $\mathbf{A}$ is a square, real and non-singular matrix, then $\mathbf{A}^{+}$ coincides with the inverse of $\mathbf{A}$, i.e., $\mathbf{A}^{+} = \mathbf{A}^{-1}$. Using the MP inverse, a closed form solution to the algebraic system of Eq. (61) is attained. In this regard, for any matrix $\mathbf{A} \in \mathbb{R}^{m\times n}$, Eq. (61) yields

$$\mathbf{x} = \mathbf{A}^{+}\mathbf{b} + (\mathbf{I}_n - \mathbf{A}^{+}\mathbf{A})\mathbf{y}, \tag{63}$$

where $\mathbf{y}$ denotes an arbitrary n-dimensional vector and $\mathbf{I}_n$ represents the $n \times n$ identity matrix. A more detailed presentation of the topic can be found in [38] and [39].

References

[1] J. Li, J. Chen, Stochastic dynamics of structures, John Wiley & Sons, 2009.

[2] P. D. Spanos, G. Failla, Wavelets: Theoretical concepts and vibrations related applications, The Shock and Vibration Digest 37 (5) (2005) 359–376.

[3] I. A. Kougioumtzoglou, I. Petromichelakis, A. F. Psaros, Sparse representations and compressive sampling approaches in engineering mechanics: A review of theoretical concepts and diverse applications, Probabilistic Engineering Mechanics 61 (2020) 103082.

[4] A. Kareem, T. Kijewski, Time-frequency analysis of wind effects on structures, Journal of Wind Engineering and Industrial Aerodynamics 90 (12-15) (2002) 1435–1452.

[5] B. Basu, V. K. Gupta, Non-stationary seismic response of mdof systems by wavelet transform, Earthquake Engineering & Structural Dynamics 26 (12) (1997) 1243–1258.

[6] A. F. Psaros, I. Petromichelakis, I. A. Kougioumtzoglou, Wiener path integrals and multi-dimensional global bases for non-stationary stochastic response determination of structural systems, Mechanical Systems and Signal Processing 128 (2019) 551–571.

[7] T. Kijewski, A. Kareem, Wavelet transforms for system identification in civil engineering, Computer-Aided Civil and Infrastructure Engineering 18 (5) (2003) 339–355.

[8] P. D. Spanos, G. Failla, A. Santini, M. Pappatico, Damage detection in euler–bernoulli beams via spatial wavelet analysis, Structural Control and Health Monitoring: The Official Journal of the International Association for Structural Control and Monitoring and of the European Association for the Control of Structures 13 (1) (2006) 472–487.

[9] B. Basu, S. Nagarajaiah, A. Chakraborty, Online identification of linear time-varying stiffness of structural systems by wavelet analysis, Structural Health Monitoring 7 (1) (2008) 21–36.

[10] I. A. Kougioumtzoglou, K. R. M. dos Santos, L. Comerford, Incomplete data based parameter identification of nonlinear and time-variant oscillators with

fractional derivative elements, Mechanical Systems and Signal Processing 94 (2017) 279–296.

[11] K. R. M. dos Santos, O. Brudastova, I. A. Kougioumtzoglou, Spectral identification of nonlinear multi-degree-of-freedom structural systems with fractional derivative terms based on incomplete non-stationary data, Structural Safety 86 (2020) 101975.

[12] P. D. Spanos, G. Failla, Evolutionary spectra estimation using wavelets, Journal of Engineering Mechanics 130 (8) (2004) 952–960.

[13] P. D. Spanos, J. Tezcan, P. Tratskas, Stochastic processes evolutionary spectrum estimation via harmonic wavelets, Computer Methods in Applied Mechanics and Engineering 194 (12-16) (2005) 1367–1383.

[14] L. Comerford, I. A. Kougioumtzoglou, M. Beer, Compressive sensing based stochastic process power spectrum estimation subject to missing data, Probabilistic Engineering Mechanics 44 (2016) 66–76.

[15] Y. Zhang, L. Comerford, I. A. Kougioumtzoglou, M. Beer, Lp-norm minimization for stochastic process power spectrum estimation subject to incomplete data, Mechanical Systems and Signal Processing 101 (2018) 361–376.

[16] P. D. Spanos, I. A. Kougioumtzoglou, Harmonic wavelets based statistical linearization for response evolutionary power spectrum determination, Probabilistic Engineering Mechanics 27 (1) (2012) 57–68.

[17] I. A. Kougioumtzoglou, Stochastic joint time–frequency response analysis of nonlinear structural systems, Journal of Sound and Vibration 332 (26) (2013) 7153–7173.

[18] D. E. Newland, Harmonic and musical wavelets, Proceedings of the Royal Society of London. Series A: Mathematical and Physical Sciences 444 (1922) (1994) 605–620.

[19] F. Kong, P. D. Spanos, J. Li, I. A. Kougioumtzoglou, Response evolutionary power spectrum determination of chain-like mdof non-linear structural systems via harmonic wavelets, International Journal of Non-Linear Mechanics 66 (2014) 3–17.

[20] I. A. Kougioumtzoglou, P. D. Spanos, Harmonic wavelets based response evolutionary power spectrum determination of linear and non-linear oscillators with fractional derivative elements, International Journal of Non-Linear Mechanics 80 (2016) 66–75.

[21] P. D. Spanos, F. Kong, J. Li, I. A. Kougioumtzoglou, Harmonic wavelets based excitation-response relationships for linear systems: A critical perspective, Probabilistic Engineering Mechanics 44 (2016) 163–173. doi:10.1016/j.probengmech.2015.09.021.

[22] F. Kong, I. A. Kougioumtzoglou, P. Spanos, S. Li, Nonlinear system response evolutionary power spectral density determination via a harmonic wavelets based Galerkin technique, International Journal for Multiscale Computational Engineering 14 (3) (2016).

[23] F. Kong, Y. Zhang, Y. Zhang, Non-stationary response power spectrum determination of linear/non-linear systems endowed with fractional derivative elements via harmonic wavelet, Mechanical Systems and Signal Processing 162 (2022) 108024.

[24] G. D. Pasparakis, V. C. Fragkoulis, M. Beer, Harmonic wavelets based response evolutionary power spectrum determination of linear and nonlinear structural systems with singular matrices, Mechanical Systems and Signal Processing 149 (2021) 107203.

[25] G. Beylkin, On the representation of operators in bases of compactly supported wavelets, SIAM Journal on Numerical Analysis 29 (6) (1992) 1716–1740.

[26] M.-Q. Chen, C. Hwang, Y.-P. Shih, The computation of wavelet-Galerkin approximation on a bounded interval, International journal for numerical methods in engineering 39 (17) (1996) 2921–2944.

[27] C. Cattani, Harmonic wavelets towards the solution of nonlinear pde, Computers & Mathematics with Applications 50 (8-9) (2005) 1191–1210.

[28] X. Xiao, Y. Zhang, W. Shen, F. Kong, A stochastic analysis method of transient responses using harmonic wavelets, part 1: Time-invariant structural systems, Mechanical Systems and Signal Processing 160 (2021) 107870.

[29] F. E. Udwadia, R. E. Kalaba, Analytical dynamics: a new approach, Cambridge University Press, 2007.

[30] V. C. Fragkoulis, I. A. Kougioumtzoglou, A. A. Pantelous, Linear random vibration of structural systems with singular matrices, Journal of Engineering Mechanics 142 (2) (2016) 04015081.

[31] A. Schutte, F. Udwadia, New approach to the modeling of complex multibody dynamical systems, Journal of Applied Mechanics 78 (2) (2011) 021018.

[32] V. C. Fragkoulis, I. A. Kougioumtzoglou, A. A. Pantelous, Statistical linearization of nonlinear structural systems with singular matrices, Journal of Engineering Mechanics 142 (9) (2016) 04016063.

[33] I. A. Kougioumtzoglou, V. C. Fragkoulis, A. A. Pantelous, A. Pirrotta, Random vibration of linear and nonlinear structural systems with singular matrices: A frequency domain approach, Journal of Sound and Vibration 404 (2017) 84–101.

[34] A. Pirrotta, I. A. Kougioumtzoglou, A. Di Matteo, V. C. Fragkoulis, A. A. Pantelous, C. Adam, Deterministic and random vibration of linear systems with singular parameter matrices and fractional derivative terms, Journal of Engineering Mechanics 147 (6) (2021) 04021031.

[35] E. N. Antoniou, A. A. Pantelous, I. A. Kougioumtzoglou, A. Pirrotta, Response determination of linear dynamical systems with singular matrices: A polynomial matrix theory approach, Applied Mathematical Modelling 42 (2017) 423–440.

[36] A. D. Karageorgos, L. Moysis, V. C. Fragkoulis, I. A. Kougioumtzoglou, A. A. Pantelous, Random vibration of linear systems with singular matrices based on Kronecker canonical forms of matrix pencils, Mechanical Systems and Signal Processing 161 (2021) 107896.

[37] P. Ni, V. C. Fragkoulis, F. Kong, I. P. Mitseas, M. Beer, Response determination of nonlinear systems with singular matrices subject to combined stochastic and deterministic excitations, ASCE-ASME Journal of Risk and Uncertainty in Engineering Systems, Part A: Civil Engineering 7 (4) (2021) 04021049.

[38] S. L. Campbell, C. D. Meyer, Generalized inverses of linear transformations, SIAM, 2009.

[39] A. Ben-Israel, T. N. E. Greville, Generalized inverses: theory and applications, Vol. 15, Springer Science & Business Media, 2003.

[40] M. F. Daqaq, R. Masana, A. Erturk, D. Q. D., On the role of nonlinearities in vibratory energy harvesting: a critical review and discussion, Applied Mechanics Reviews 66 (4) (2014).

[41] I. Petromichelakis, A. F. Psaros, I. A. Kougioumtzoglou, Stochastic response determination and optimization of a class of nonlinear electromechanical energy harvesters: A Wiener path integral approach, Probabilistic Engineering Mechanics 53 (2018) 116–125.

[42] I. Petromichelakis, A. F. Psaros, I. A. Kougioumtzoglou, Stochastic response analysis and reliability-based design optimization of nonlinear electromechanical energy harvesters with fractional derivative elements, ASCE-ASME Journal of Risk and Uncertainty in Engineering Systems, Part B: Mechanical Engineering 7 (1) (2021) 010901.

[43] S. Adhikari, M. I. Friswell, D. J. Inman, Piezoelectric energy harvesting from broadband random vibrations, Smart Materials and Structures 18 (11) (2009) 115005.

[44] I. Petromichelakis, A. F. Psaros, I. A. Kougioumtzoglou, Stochastic response determination of nonlinear structural systems with singular diffusion matrices: A Wiener path integral variational formulation with constraints, Probabilistic Engineering Mechanics 60 (2020) 103044 1–15.

[45] J. Liang, S. R. Chaudhuri, M. Shinozuka, Simulation of nonstationary stochastic processes by spectral representation, Journal of Engineering Mechanics 133 (6) (2007) 616–627.

[46] J. B. Roberts, P. D. Spanos, Random vibration and statistical linearization, Courier Corporation, 2003.

[47] A. F. Psaros, O. Brudastova, G. Malara, I. A. Kougioumtzoglou, Wiener path integral based response determination of nonlinear systems subject to non-white, non-Gaussian, and non-stationary stochastic excitation, Journal of Sound and Vibration 433 (2018) 314–333.

[48] T. Kijewski, A. Kareem, On the presence of end effects and their melioration in wavelet-based analysis, Journal of Sound and Vibration 256 (5) (2002) 980–988.

[49] F. E. Udwadia, T. Wanichanon, On general nonlinear constrained mechanical systems, Numer. Algebra Control Optim 3 (3) (2013) 425–443.

[50] V. C. Fragkoulis, I. A. Kougioumtzoglou, A. A. Pantelous, M. Beer, Joint statistics of natural frequencies corresponding to structural systems with singular random parameter matrices, Journal of Engineering Mechanics (2022) 10.1061/(ASCE)EM.1943–7889.0002081.

[51] L. Mariti, N. P. Belfiore, E. Pennestrì, P. P. Valentini, Comparison of solution strategies for multibody dynamics equations, International Journal for Numerical Methods in Engineering 88 (7) (2011) 637–656.

[52] P.-T. D. Spanos, G. P. Solomos, Markov approximation to transient vibration, Journal of Engineering Mechanics 109 (4) (1983) 1134–1150.

[53] V. C. Fragkoulis, I. A. Kougioumtzoglou, A. A. Pantelous, M. Beer, Nonstationary response statistics of nonlinear oscillators with fractional derivative elements under evolutionary stochastic excitation, Nonlinear Dynamics 97 (4) (2019) 2291–2303.

[54] Z. C. He, Z. Zhang, E. Li, Multi-source random excitation identification for stochastic structures based on matrix perturbation and modified regularization method, Mechanical Systems and Signal Processing 119 (2019) 266–292.